

Resonance-induced quenching of luminescence and reduction of tunneling time in $\text{Al}_x\text{Ga}_{1-x}\text{As}/\text{GaAs}$ multiple-quantum-well structures

S. Tarucha,* K. Ploog, and K. von Klitzing

Max-Planck-Institut für Festkörperforschung, D-7000 Stuttgart 80, Federal Republic of Germany

(Received 30 March 1987)

We have observed a strong reduction of the tunneling time in a $\text{Al}_{0.29}\text{Ga}_{0.71}\text{As}(5.8\text{ nm})/\text{GaAs}(12\text{ nm})$ multiple-quantum-well structure caused by resonances of electrons between the first excited state and the ground state (down to 430 ps) and also between the second excited state and the ground state (down to less than 60 ps), which are adjusted by electric fields. In addition, we provide evidence for the quenching of the excitonic luminescence to be also induced by the resonance from a comparison of the tunneling time and the recombination time.

Recent developments in the growth of artificially layered structures have made feasible the extensive study of tunneling effects in semiconductor superlattices or multiple-quantum-well structures (MQWS's). Most of the resonant-tunneling features in the superlattices were exemplified in static current-voltage characteristics.¹ Recently, a striking evidence for resonant tunneling was provided by the observation of two peaks in the low-temperature photocurrent-voltage characteristics of a $\text{Al}_x\text{In}_{1-x}\text{As}/\text{Ga}_x\text{In}_{1-x}\text{As}$ MQWS.² These peaks were attributed to resonance of electrons between the first two excited states and the ground state in the adjacent wells.³ A similar resonance feature was also observed in a $\text{Al}_x\text{Ga}_{1-x}\text{As}/\text{GaAs}$ MQWS.⁴ As yet, however, only very few studies of the dynamical aspects of resonant tunneling have been reported, although a considerable interest in the effect of resonance on tunneling times exists. The measured time-resolved photocurrent (PC) of a MQWS at room temperature showed a remarkable decrease of the decay time due to the tunneling of carriers, but a resonance effect was not observed.^{5,6} The tunneling properties were also studied by measurements of excitonic photoluminescence (PL) in QW heterostructures^{7,8} and MQWS's.⁹⁻¹¹ A comparison of PL and PC at low temperatures revealed an excess PC generated by the field-induced ionization of exciton.^{7,11} The time-resolved PL of a QW with thick barriers exhibited a decrease of the carrier lifetime in high fields due to tunneling.^{8,10} Recently, in a $\text{Al}_x\text{Ga}_{1-x}\text{As}/\text{GaAs}$ MQWS with rather thick barriers, a constant fast decay of the excitonic PL was observed in low fields and attributed to the resonant-tunneling effect.¹¹

In this paper we report the observation of the reduction of the tunneling time in a $\text{Al}_x\text{Ga}_{1-x}\text{As}/\text{GaAs}$ MQWS caused by resonance effects of electrons between the first excited state and the ground state (down to 430 ps) and also between the second excited state and the ground state (down to less than 60 ps) in the respective adjacent wells. In addition, we provide direct evidence for the quenching of the excitonic PL induced by the resonance effect from a comparison of the tunneling time and the excitonic recombination time. Time-resolved PC as well as static PL and PC measurements are used to study the tunneling properties of the $\text{Al}_x\text{Ga}_{1-x}\text{As}/\text{GaAs}$ MQWS. The exciting en-

ergy is chosen to be slightly higher than the energies of the excitonic absorption peaks at the energy gap, in order to generate carriers homogeneously in the entire MQWS region along the axis of the layer sequence.

The sample is a *p-i-n* heterostructure diode grown by molecular-beam epitaxy. The intrinsic region consists of a 100-period $\text{Al}_{0.29}\text{Ga}_{0.71}\text{As}(5.8\text{ nm})/\text{GaAs}(12\text{ nm})$ MQWS and is sandwiched between 1- μm -thick $\text{Al}_{0.49}\text{Ga}_{0.51}\text{As}$ layers doped with Si to $n=2\times 10^{17}\text{ cm}^{-3}$ and with Be to $p=1\times 10^{18}\text{ cm}^{-3}$, respectively. The diode is processed into a high mesa-type cylindrical geometry having a diameter of 190 μm . A cutoff frequency of 10 GHz is derived from the RC time constant. A built-in voltage of the diode is evaluated to be 1.6 V at 20 K from the PC-voltage characteristics. The time-resolved PC is measured using a 785-nm $\text{Al}_x\text{Ga}_{1-x}\text{As}$ double-heterostructure laser diode as exciting light source. Optical pulses of 200 ps duration and 100 kHz repetition rate are generated by injecting electric pulses into the laser diode. The peak excitation density is estimated to be about 0.5 W cm^{-2} . The absorption coefficient is about 10^{-2} per well at 785 nm.¹² The time-resolved PC is measured with a 14-GHz sampling oscilloscope combined with a computer system to integrate the signal. dc voltages are bandwidth limited between 10 kHz and 18 GHz. The overall time resolution of the detection system is approximately 40 ps. The PC signal is fed from the sample mounted in a cryostat to the sampling oscilloscope through a semirigid cable. Due to the heat dissipation of the semirigid cable the lowest temperature achieved on the sample is 20 K. Static PL and PC measurements are performed with the sample cooled to 5 K using the cw 753-nm line of a Kr^+ laser with about 5 W cm^{-2} .

Figure 1 shows the static PC and the spectrally integrated PL intensity versus bias voltage measured under the same excitation conditions. The negative sign of the bias voltage V_b denotes the backward of the diode. The observed PL is associated with excitons of electrons and heavy holes in the ground states.¹¹ The PL intensity shows a small dip labeled *A* and a large dip labeled *C* at $V_b = -3.2$ and -9 V, respectively, and a complete quenching for $V_b < -16$ V. At the same voltages as the dips *A* and *C* the PC shows small peaks *a* and *c*, and also a broad peak *d* at -17 V, where the PL intensity is com-

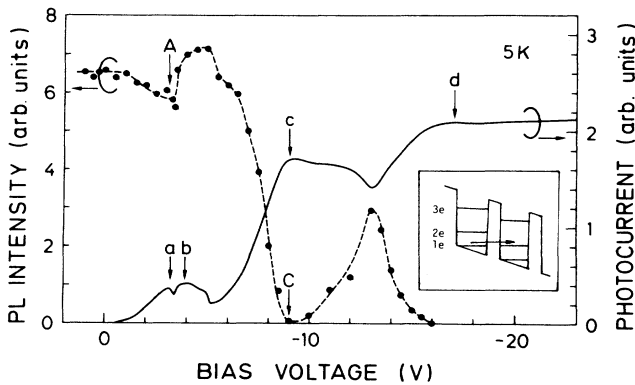


FIG. 1. Static PC and integrated PL intensity vs bias voltage. The arrows indicate the peaks of the PC and the dips of the PL intensity. The broken line is a guide for the eyes. The inset shows a sketch of the resonance between $2e$ and $1e$.

pletely quenched. This correspondence indicates that the peaks a , c , and d are induced by the carriers generated by the field ionization of excitons and are thus associated with the escape of electrons or heavy holes in the ground states from the wells.^{7,11} The effective-mass calculation of the energy levels leads to the assignment of the peaks c and d to resonance effects of electrons between the first two excited states and the ground state.^{2,4} The electric field across each constituent MQWS period, which is evaluated from the Stark shift of the PL emission energy to eliminate the field-screening effect of the photogenerated carriers,¹¹ amounts to 13, 37, and 80 kVcm^{-1} for the peaks a , c , and d , respectively.¹³ The calculation yields the energy difference of 65 meV between the first excited electron state ($2e$) and the ground electron state ($1e$) and 161 meV between the second excited electron state ($3e$) and $1e$.¹⁴ These values predict resonances at 37 and 90 kVcm^{-1} , which are in good agreement with those for the peaks c and d , respectively. In the same manner we attribute the peak a to resonance between the first excited heavy-hole state (2HH) and the ground heavy-hole state (1HH) or between 1HH and the ground light-hole state (1LH). The effective-mass calculation predicts resonance between 2HH and 1HH at 8 kVcm^{-1} and resonance between 1HH and 1LH at 7 kVcm^{-1} .¹⁴ These values are in good agreement with the measured data of the peak a , although no significant feature to distinguish the two resonance effects is observed. The PC shows another small peak b at -3.9 V, which is accompanied by a slight increase of the PL intensity in contrast to the other three peaks. We therefore assume that this peak is either due to the quenching of a nonradiative recombination process associated with residual impurities or defects or due to the field-induced change of the absorption coefficient at the exciting energy. The excellent correspondence between the PL intensity and the PC in Fig. 1 indicates that the injection of carriers in the MQWS contributes either to the luminescence or to the photocurrent. The dips of the PL intensity imply the quenching caused by resonance effects. We discuss the competitive processes of excitonic recombination and resonant tunneling again in connection with

the time-resolved PC characteristics.

In Figs. 2(a) and 2(b) we show the time-resolved PC obtained at different bias voltages. The periodic oscillation in the decay profile is caused by electrical reflection. For $V_b < -3$ V, remarkable changes in the PC decay profile are observed. The time-resolved PC exhibits two different exponential decay components, i.e., a fast initial decay and a slow subsequent decay. The peak of the PC is followed by the fast initial decay. The peak (maximum) value of the PC (PCM) becomes first larger when V_b is decreased from -4 to -6.5 V and then smaller when V_b is further decreased down to -10 V. A similar change of PCM is observed for V_b from -10 to -15 V. PCM be-

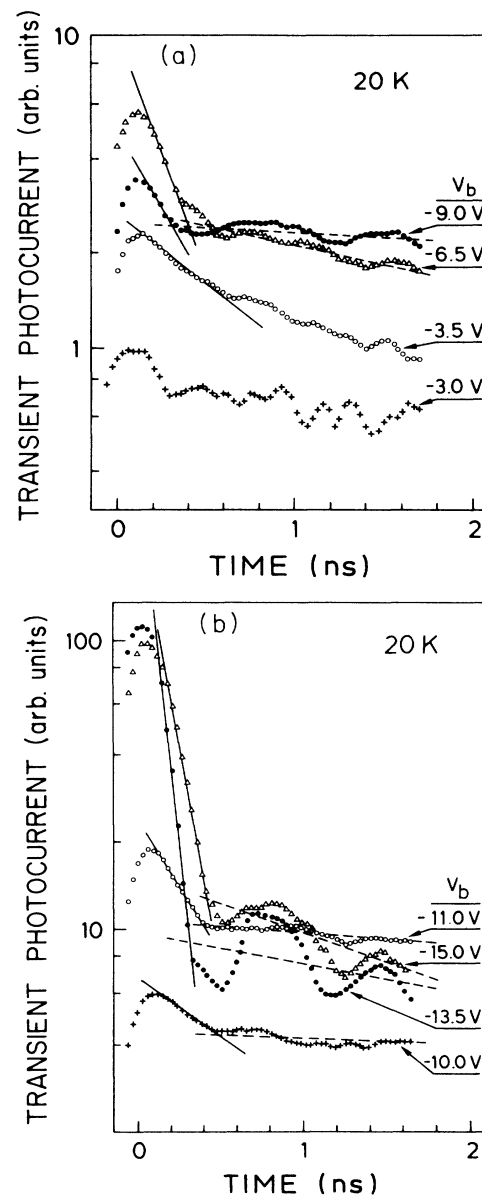


FIG. 2. Time dependence of the PC at different bias voltages: (a) -3 V $> V_b > -9$ V, (b) -10 V $> V_b > -20$ V. The solid and broken lines describe the biexponential decay.

comes larger again when V_b is further decreased down to -20 V. For $V_b > -3$ V, no difference of the time-resolved profile between the initial and the subsequent decay components are detected because of the limitation imposed by the signal-to-noise ratio.

The peak value PCM and the time constant τ_i of the initial decay components are plotted in Fig. 3 as a function of the bias voltage. The value of τ_i is determined from the slope of the initial decay as, e.g., indicated by the solid lines in Fig. 2. The value of $\tau_i = 60$ ps is the lower limit given by the time-resolved decay profile of the exciting pulse. For $V_b > -3.5$ V, τ_i is not determined for the reason given before. PCM shows three peaks at -0.8 , -6.5 , and -13.5 V following the abrupt increases in the larger V_b ranges. This feature is well reproduced in the static PC curve, i.e., the peaks at -0.8 , -6.5 , and -13.5 V are compared to the peaks *a* or *b*, *c*, and *d*, respectively, although the peaks of PCM are slightly shifted to the larger V_b ranges because the field screening is smaller under pulse excitation. The peak at -13.5 V appears more clearly than the peak *d* since PCM gives the peak value of the time-resolved PC. The electric field across the MQWS period given by $(V_0 - V_b)/t$, where V_0 is the built-in voltage and t is the total thickness of the MQWS region, is 13 kV cm^{-1} at -0.8 V, 46 kV cm^{-1} at -6.5 V, and 85 kV cm^{-1} at -13.5 V. These values are in good agreement with those of the peaks of the static PC (peak *a* or *b*, *c*, and *d*). The separation of the two peaks (*a* and *b*) is not detected in the PCM data possibly due to the limitation by the signal-to-noise ratio. At the same voltages as the peaks of PCM (-6.5 and -13.5 V) τ_i exhibits large dips. Therefore, these dips of τ_i are attributed to reso-

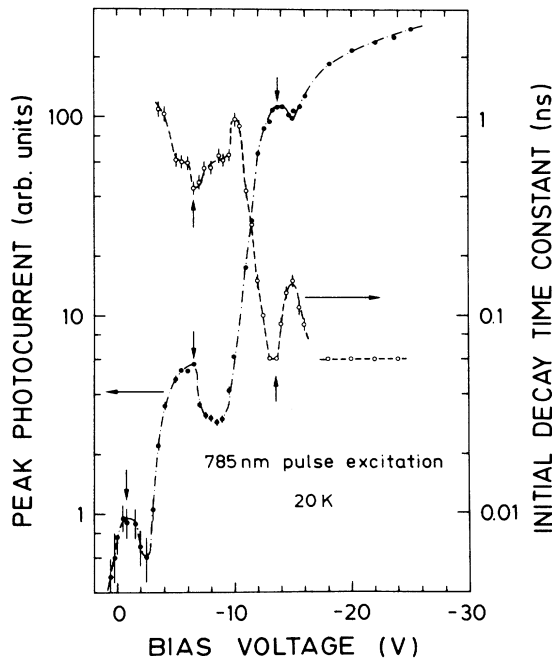


FIG. 3. Peak value PCM and time constant τ_i of the initial PC decay as a function of bias voltage. The arrows indicate the peaks of PCM and the dips of τ_i . The broken and dashed-dot lines are guides for the eyes.

nance effects of electrons between $2e$ and $1e$ (at -6.5 V) and also between $3e$ and $1e$ (-13.5 V). As far as the initial decay component of time-resolved PC is concerned, we find that the main features are well explained by assuming the tunneling of electrons. On the other hand, the subsequent decay component has a time constant of 5 – 10 ns, which can be only approximately evaluated in the measured time range. This decay may be attributed to the tunneling of holes. Additional investigations are required to trace the tunneling properties of holes in detail.

The population of carriers in the MQWS decays due to radiative recombination or due to carrier escape through the barriers as mentioned before. The carrier lifetime τ_c is given by $\tau_c^{-1} = \tau_i^{-1} + \tau_{ex}^{-1}$, where τ_i is the carrier escape time and τ_{ex} is the radiative recombination time. For the PC the relative intensity and the decay time are given by τ_c/τ_{ex} and τ_c , respectively, while for the PL they are given by τ_c/τ_{ex} and τ_c , respectively. When the electric field is increased, τ_i is reduced by the field-induced tunneling,^{5,6,8,10} while τ_{ex} is enhanced by the charge separation.⁸ Here we assume $\tau_c \approx \tau_i$. In most of the previous time-resolved PL and PC measurements a monotonic decrease of τ_c with increasing electric field was observed, and this finding could be attributed to the field-induced tunneling without considering resonance effects. The dips observed in the τ_i (Fig. 3), however, provide direct experimental evidence for a drastic reduction of the tunneling time in the MQWS caused by resonance of electrons. The symmetric V_b dependence of τ_i around the dip at -6.5 V demonstrates that the reduction of τ_i is determined only by the resonance effect and not affected by the magnitude of the electric field.

The smallest τ_i value measured in the V_b range of the resonance is 430 ps at -6.5 V and less than 60 ps around -13.5 V. This difference is attributed to the larger overlap of the wave function between $3e$ and $1e$ in the adjacent wells. For a rough estimate we assume that the overlap is related to the tunneling probability of electrons in the excited states without electric field, according to $\exp\{-[(8m_e^*/h^2)(\Delta E_c - E)]^{1/2}L_B\}$, where m_e^* is the electron effective mass and ΔE_c is the conduction-band discontinuity, E is the confinement energy of the excited states, and L_B is the barrier thickness. As this formula reflects the extension of the wave function from one well to the next one, we can approximate the ratio of the tunneling probabilities associated with $2e$ and $3e$ within the order of magnitude. The calculated ratio is 0.08 , which compares favorably with the value of < 0.14 (less than 60 ps divided by 430 ps) given by the measured τ_i . The parameters given in Ref. 14 and E evaluated from our static PC and PL measurement are used.

Of particular interest is the behavior of the time constant τ_i for V_b less than -14 V. τ_i becomes smaller when V_b is decreased below -15 V. This reduction of τ_i is associated with the tunneling of electrons from the ground state in the wells to continuum states in the neighboring wells because $3e$ evaluated from the resonance peak of the static PC curve is only 10 – 20 meV below the top of the potential barrier. This interpretation ensures the validity of our assumption that $\Delta E_c = 0.62$ (energy-gap difference).

The quenching of the static PL intensity shown in Fig. 1 is well explained by comparing the field dependence of τ_c and τ_{ex} . In the low-field range τ_{ex} is 1.5 ns, as reported previously,¹¹ and it increases gradually with increasing electric field.⁸ The τ_c is given by the τ_i shown in Fig. 3. When the electric field is close to the value providing the resonance between $2e$ and $1e$, τ_c is reduced down to 430 ps. This value is sufficiently small to quench the PL intensity given by τ_c/τ_{ex} . However, when V_b is further decreased, τ_c becomes as large as 1 ns, which is comparable to τ_{ex} so that the PL intensity recovers. The PL intensity best recovered for $V_b < -10$ V is one-third of the intensity observed for $V_b > 0$ V. This finding is in good agreement with the value of $\tau_c/\tau_{ex} \approx \frac{1}{3}$, where the enhancement of τ_{ex} is taken into account by a factor of 2.⁸ When V_b is further decreased and approaches the value giving the resonance of electrons between $3e$ and $1e$, τ_c becomes abruptly small, leading to the relation of $\tau_c \ll \tau_{ex}$, which means the complete PL quenching.

In conclusion, we use time-resolved PC measurements as well as static PL and PC measurements to study the

tunneling properties of a $\text{Al}_{0.29}\text{Ga}_{0.71}\text{As}/\text{GaAs}$ MQWS forming the intrinsic region of a p - i - n heterostructure diode in detail. The carriers are generated homogeneously in the entire MQWS region due to the appropriate choice of the exciting light energy. A strong reduction of the electron tunneling time is observed which is caused by resonance effects between $2e$ and $1e$ (down to 430 ps) and also between $3e$ and $1e$ (down to less than 60 ps) in the respective adjacent wells. In addition, from a comparison of the tunneling time and the excitonic recombination time, direct evidence is given for the resonance-induced quenching of the excitonic luminescence.

Part of this work was sponsored by the Stiftung Volkswagenwerk and by the Bundesministerium für Forschung und Technologie of the Federal Republic of Germany. The authors are grateful to A. Fischer and B. Ullrich for technical assistance with the PC measurement, to Dr. H.-J. Polland for critical reading of the manuscript, and to Dr. H. Okamoto for fruitful discussions.

*Permanent address: Nippon Telegraph and Telephone Corporation, Electrical Communications Laboratories, Tokyo 180, Japan.

¹L. Esaki, L. L. Chang, W. E. Howard, and V. L. Rideout, in *Proceedings of the Eleventh International Conference on the Physics of Semiconductors, Warsaw, Poland, 1972*, edited by The Polish Academy of Sciences (PWN-Polish Scientific Publishers, Warsaw, Poland, 1972), p. 431.

²F. Capasso, K. Mohammed, and A. Y. Cho, *Appl. Phys. Lett.* **48**, 478 (1986).

³R. F. Kazarinov and R. A. Suris, *Fiz. Tekh. Poluprovodn.* **5**, 797 (1971) [*Sov. Phys. Semicond.* **5**, 707 (1971)].

⁴T. Furuta, K. Hirakawa, I. Yoshino, and H. Sakaki, *Jpn. J. Appl. Phys.* **25**, L151 (1986).

⁵A. Larsson, A. Yariv, R. Tell, J. Maserjian, and S. T. Eng, *Appl. Phys. Lett.* **47**, 866 (1985).

⁶T. H. Wood, C. A. Burrus, A. H. Gnauck, and J. M. Wiesenfeld, D. A. B. Miller, D. S. Chemla, and T. C. Damen, *Appl. Phys. Lett.* **47**, 190 (1985).

⁷Y. Horikoshi, A. Fischer, and K. Ploog, *Phys. Rev. B* **31**, 7859 (1985).

⁸H.-J. Polland, K. Kohler, L. Schultheis, J. Kuhl, E. O. Gobel, and C. W. Tu, *Superlattices Microstruct.* **2**, 309 (1986).

⁹E. E. Mendez, G. Bastard, L. L. Chang, and L. Esaki, *Phys. Rev. Lett.* **26**, 7101 (1982).

¹⁰J. A. Kash, E. E. Mendez, and H. Morkoc, *Appl. Phys. Lett.* **46**, 173 (1985).

¹¹Y. Masumoto, S. Tarucha, and H. Okamoto, *Phys. Rev. B* **33**, 5961 (1986).

¹²H. Iwamura, T. Saku, and H. Okamoto, *Jpn. J. Appl. Phys.* **24**, 104 (1985).

¹³The emission energy is interpolated for the peak c and extrapolated for the peak d from the values at voltages close to the individual peaks because of the difficulty in determining the emission energy of the extremely weak PL precisely. The evaluated Stark shifts are 0.3, 0.6, 3.9, and 20.5 meV for the peaks a , b , c , and d , respectively.

¹⁴We followed the calculation of energy levels in a finite well by Bastard. [See G. Bastard and J. A. Brum, *IEEE J. Quantum Electron.* **QE-22**, 1625 (1986).] The effective masses used in the calculation are $0.45m_0$ for heavy holes and $0.08m_0$ for light holes. For electrons the effective mass given by $m_e^*(0)(1 + (E/E_g)\{1 - [m_e^*(0)/m_0]\}^2)$ is used to take into account the nonparabolicity of the conduction band. E is the confinement energy of electrons in quantum wells, and the effective mass $m_e^*(0)$ and the band gap E_g in the bulk GaAs are $0.0665m_0$ and 1.519 eV, respectively. A 62%–38% rule is chosen for the band discontinuity. The calculated energies of $1e$, $2e$, and $3e$ are 22.5, 86.9, and 180.8 meV, respectively, and those of 1HH, 2HH, and 1LH are 4.6, 18.1, and 17.5 meV, respectively at zero field. The energy shifts at finite fields are calculated for the ground states as described in Ref. 11, whereas those for the excited states are neglected.